

Supplementary Information

Programming Microbe-Computer Interaction for Customized Life-Nonlife and Cross-Life Communication

Figure S1. Expansion of MCU functions for detecting the sampled bioluminescent bacteria.

Figure S2. Assembly of the stent-form CMU actuator and electrical test.

Figure S3. Test of opto-activation of microbial protein expression using stent-form CMU actuator.

Table S1. The engineered microbial strains in this study.

Table S2. The constructed plasmids in this study.

Movie S1. Implantation of CMU stent in live pig rectum.

Movie S2. Endoscopic visualization of CMU stent implantation in live pig rectum.

Movie S3. Endoscopic visualization of the externally-controlled LED switching.

Movie S4. Simulation of the USV sampling, sensing and activating the alert LED.

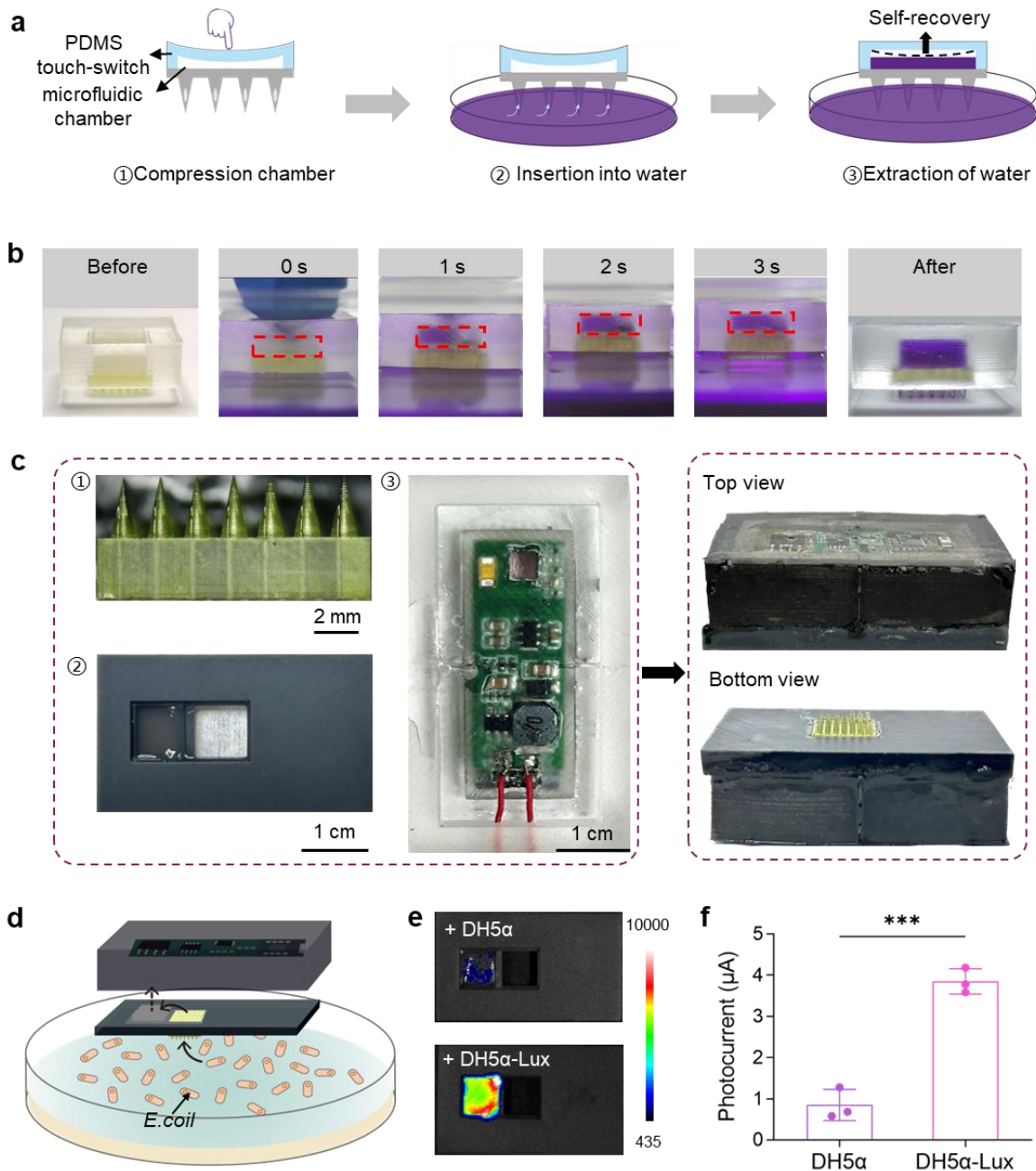


Figure S1. Expansion of MCU functions for detecting the sampled bioluminescent bacteria.

a, Diagram of the sample uptake process using a touch-switch microfluidic chamber. **b**, Photographs of the chamber in **a** and the sample uptake process. **c**, Illustration of assembling MCU unit consisting of the microneedle, light-proof enclosure, and integrated electronic circuit board. **d**, Illustration of sampling from the liquid containing *E. coli* strains through the microneedle interface of the MCU unit. **e**, Imaging of bioluminescence after respective uptake of different strains using the setup in **d**. **f**, Photocurrent detection results of the experiment in **d**. All the

measurements were taken from three distinct biological replicates. Significance was determined by unpaired two-tailed Student's t-test for **f**. * $0.01 < p < 0.05$, ** $0.001 < p < 0.01$, *** $p < 0.001$.

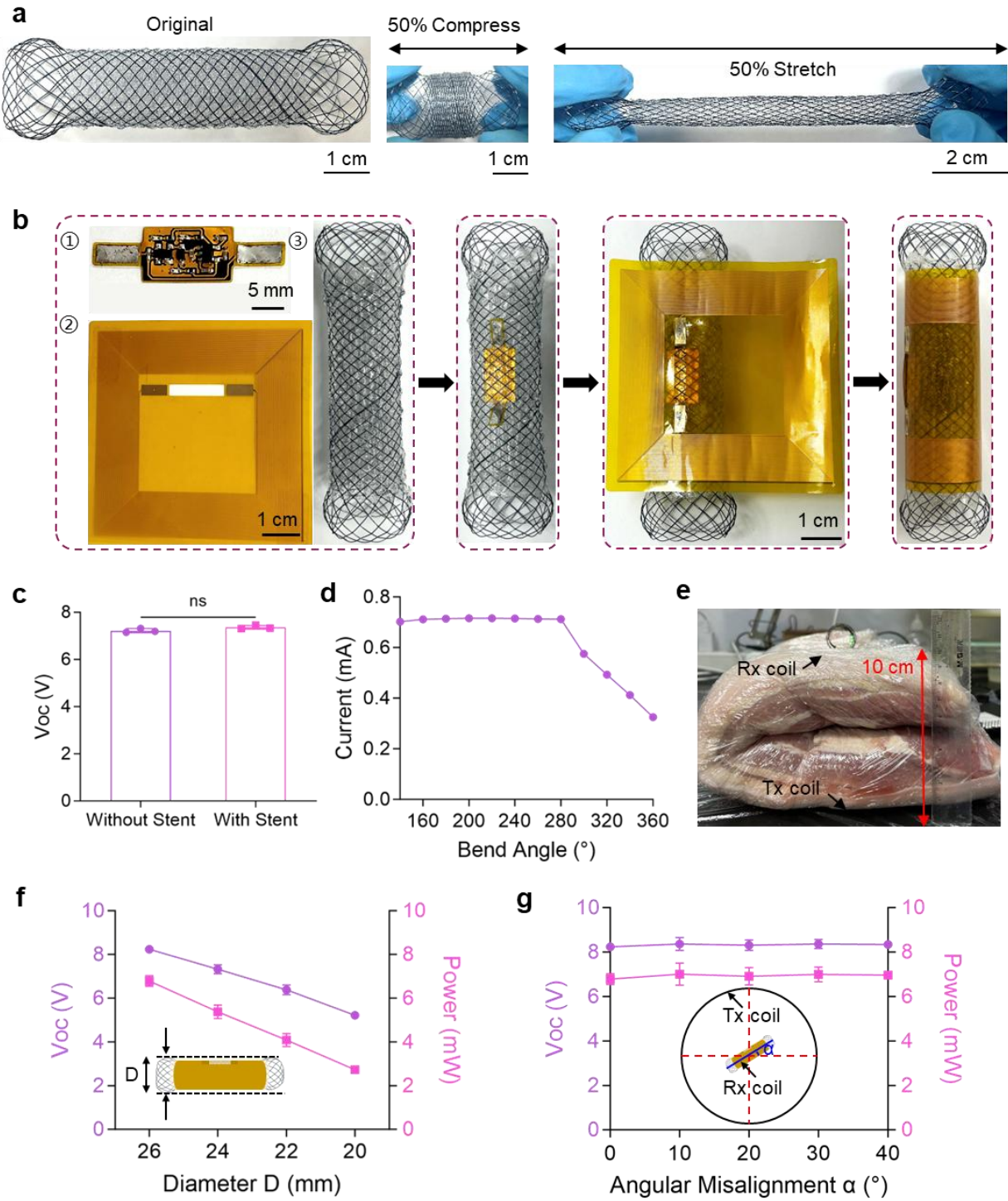


Figure S2. Assembly of the stent-form CMU actuator and electrical test. **a**, Feasibility test of 50% compression or 50% stretching of a stent encapsulated with biocompatible PVA material. **b**, Photograph of the fully assembled stent-configured MCU, consisting of the PVA layer (pre-loaded with optogenetic engineered bacteria as needed), stent structure, and electronic modules. **c**,

Measurement of the open-circuit voltage of the receiving coil under different stent configurations. **d**, Effect of bending angle of the receiving coil on the operating current of the electronic circuit. **e**, Diagram of the experimental setup for wirelessly charging the MCU stent through a 10 cm-thick porcine tissue section using an external transmitter (Tx) coil and evaluating circuit performance. **f**, Test of the variations in open-circuit voltage and output power of the electronic circuit under stent compression. **g**, Test of the variations in open-circuit voltage and output power of the electronic circuit as the stent is rotated at different angles relative to the transmitter coil. Significance was determined by unpaired two-tailed Student's t-test for **c**.

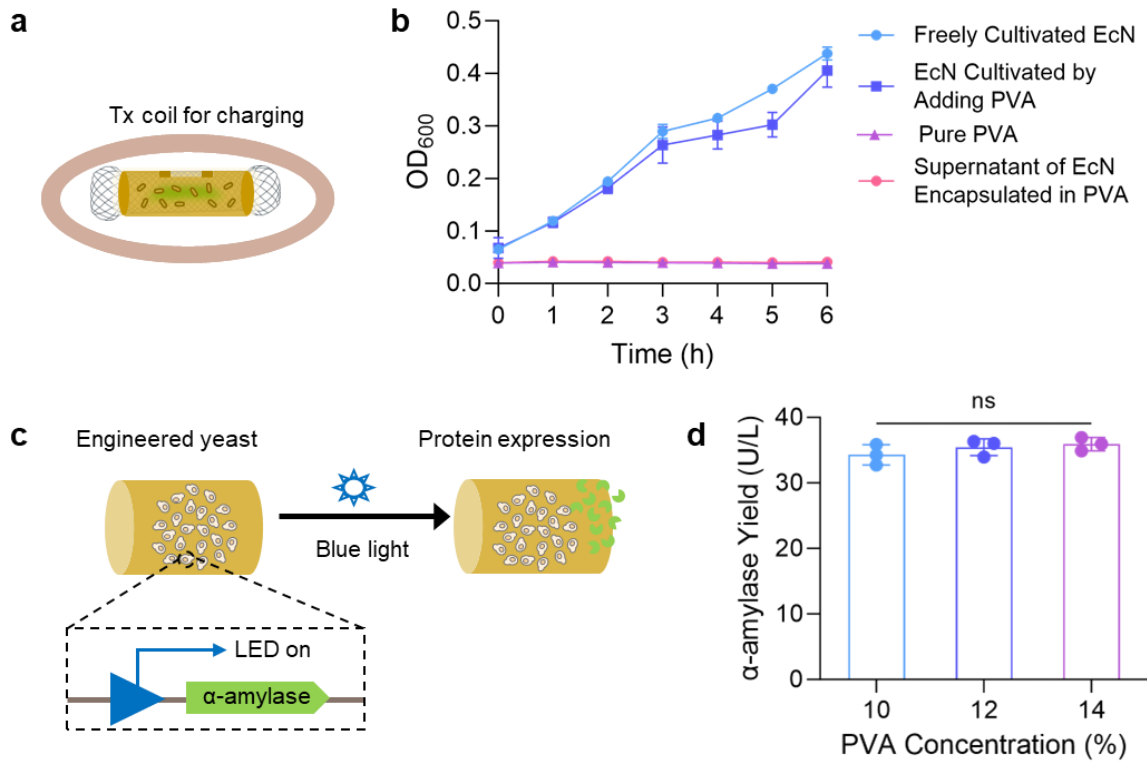


Figure S3. Test of opto-activation of microbial protein expression using stent-form CMU actuator. **a**, Diagram of wireless charging and activation of the stent-formed MCU actuator via a Tx coil. **b**, Test of the effect of PVA material on the growth performance of engineered EcN bacteria in culture medium, along with the assessment of potential bacterial leakage from PVA-encapsulated EcN. **c**, Diagram of the activation of α -amylase expression in PVA-encapsulated engineered yeast upon LED switching. **d**, Effect of varying PVA concentrations on the expression and secretion of α -amylase in encapsulated yeast. All the measurements were taken from three distinct biological replicates. Significance was determined by one-way ANOVA with Dunnett's post-test for **d**.

Table S1. The engineered microbial strains in this study.

Name	Key characteristics
EcN	<i>E. coli</i> Nissle 1917 Δ pMUT1 Δ pMUT2 (cryptic plasmids)
<i>B. subtilis</i> 168	ATCC 23857, Ind ⁻ Tyr ⁺
<i>S. cerevisiae</i> BY4741	MATa his3 Δ 1 leu2 Δ 0 met15 Δ 0 ura3 Δ 0
EcN-CSG-Lux	EcN Δ csgA, Δ csgD::pJ23101-csgEFG, pJ23100-csgBC, Δ lacZ::pJ23100-LuxABCDE
DH5 α -Lux	DH5 α harboring pCons-LuxABCDE
<i>B. subtilis</i> -Lux	<i>B. subtilis</i> 168 integrated with Ppen-luxABCDE cistron at wprA site
<i>S. cerevisiae</i> BY4741-Lux	<i>S. cerevisiae</i> BY4741 transformed with pRS425 plasmid inserted by P _{TEF1} -nanoluc-T _{GPM1}
DH5 α -Ara	DH5 α transformed with pAra-LuxABCDE
EcN-Nitrate	EcN-CSG-Lux transformed with pNitrate-LuxA
EcN-Tet	EcN-CSG-Lux transformed with pTet-LuxA
EcN-Heme	EcN-CSG-Lux transformed with pHeme-LuxA
DH5 α -Hypoxia	DH5 α transformed with pHypoxia-LuxCDABE
EcN-Pb	EcN-CSG-Lux transformed with pPb-LuxA
EcN-As	EcN-CSG-Lux transformed with pAs-LuxA
EcN-Opto-GFP	EcN harboring p15A-ccaS-PCB and pGreen-sfGFP
EcN-Opto-Lux	EcN-CSG-Lux harboring p15A-ccaS-PCB and pGreen-LuxA
EcN-Opto-secGFP	EcN harboring pHlyBD, p15A-ccaS-PCB and pGreen-sfGFP-H60
EcN-Opto-secCherry	EcN harboring pHlyBD, p15A-ccaS-PCB and pGreen-mCherry-H60
EcN-Opto-secPD-L1nb	EcN harboring pHlyBD, p15A-ccaS-PCB and pGreen-Nb-PD-L1nb-H60
EcN-Opto-secMtnB	EcN harboring pHlyBD, p15A-ccaS-PCB and pGreen-Nb-MtnB-H60
EcN-Opto-secIL-10	EcN harboring pHlyBD, p15A-ccaS-PCB and pGreen-Nb-IL-10-H60

BY4741-Opto-
secAmylase

S. cerevisiae BY4741 harboring pBlue-Amylase

Table S2. The constructed plasmids in this study.

Name	Key characteristics
pCons-LuxABCDE	p15A ori, Kan ^R , T5- <i>luxABCDE</i>
pAra-LuxABCDE	p15A ori, Chl ^R , P _{BAD} - <i>luxABCDE</i> , P _C - <i>AraC</i>
pNitrate-LuxA	pRSF ori, Amp ^R , P _{YeaR} -Toehold switch- <i>luxA</i> , P _{YeaR} -Trigger
pTet-LuxA	p15A ori, Kan ^R , P _{JKR} -tetR-P _{LtetO} - <i>luxA</i>
pHeme-LuxA	Plasmid 1: P _{J23104} - <i>chuA</i> , P _{taco2} - <i>luxC-lacI</i> , P _{J23100} - <i>hrtR</i> ; Plasmid 2: P _{tac} - <i>luxA-luxB</i> , P _{tac} - <i>luxD-luxE</i>
pHypoxia-LuxCDABE	pYfiD- <i>luxCDABE</i>
pPb-LuxA	pRSF ori, Amp ^R , P
pAs-LuxA	p15A ori, Kan ^R , P _{probe-NT} , P _{lacV} - <i>arsR</i> , P _{arsOC2} - <i>luxA</i>
p15A-ccaS-PCB	p15A ori, Chl ^R , P _{J23106} - <i>mini ccaS</i> , P _{J23108} - <i>HOI-pcyA-L3S1P22</i>
pGreen-GFP	pUC ori, Kan ^R , P _{J23100} - <i>ccaR</i> -T _{B0015} , P _{cpcG2} - <i>sfGFP</i> -T _{rrnB}
pGreen-luxA	pUC ori, Kan ^R , P _{J23100} - <i>ccaR</i> -T _{B0015} , P _{cpcG2} - <i>luxA</i> -T _{rrnB}
pHlyBD	pSC101 ori, Amp ^R , P _{J23100} - <i>HlyBD</i> -T _{B0015}
pGreen-GFP-H60	pUC ori, Kan ^R , P _{J23100} - <i>ccaR</i> -B0015, P _{cpcG2} - <i>sfGFP-H60</i> -rrnB T1
pGreen-mCherry-H60	pUC ori, Kan ^R , P _{J23100} - <i>ccaR</i> -B0015, P _{cpcG2} - <i>sfGFP-H60</i> -rrnB T1
pGreen-PD-L1nb-H60	pUC ori, Kan ^R , P _{J23100} - <i>ccaR</i> -B0015, P _{cpcG2} - <i>PD-L1nb-H60</i> -rrnB T1
pGreen-MtnB-H60	pUC ori, Kan ^R , P _{J23100} - <i>ccaR</i> -B0015, P _{cpcG2} - <i>MtnB-H60</i> -rrnB T1
pGreen-IL-10-H60	pUC ori, Kan ^R , P _{J23100} - <i>ccaR</i> -B0015, P _{cpcG2} - <i>IL-10-H60</i> -rrnB T1
pBlue-Amylase	Plasmid 1: pRS425-P _{TEF1} -CIBN-T _{ADH1} -P _{GAP} -CRY2-T _{GPM1} ; Plasmid 2: pRS413-EL222-nanoluc

Movie S1. Implantation of CMU stent in live pig rectum.

Movie S2. Endoscopic visualization of CMU stent implantation in live pig rectum.

Movie S3. Endoscopic visualization of the externally-controlled LED switching.

Movie S4. Simulation of the USV sampling, sensing and activating the alert LED.